SUPPLEMENTAL MATERIALS

Supplemental methods

Human subjects

Pregnant women receiving care at the Stanford Obstetrics Clinic were enrolled in this study after written informed consent with an approved protocol from the Stanford University Institutional Review Board. A total of 25 preeclamptic subjects (n=25) and 34 gestational age-matched normal subjects (n=34) without PE or any other pregnancy complications were recruited. The details of subject selection and clinical diagnosis of PE have been published previously (1, 2). PE was defined as systolic blood pressure of $\geq$140 or diastolic blood pressure $\geq$ 90 mm Hg more than once and significant proteinuria ($\geq$ 300 mg/24 h, 1+ on dipstick, or urine protein/creatinine ratio of $\geq$ 0.19) (1, 2). Placental bed biopsies and full-thickness placental samples from the central basal plate area were collected at the time of delivery and processed for in situ hybridization (ISH) studies, as described previously (1).

Endometrium-specific gene delivery in mice

We compared different methods for gene delivery into the uterus using adenovirus and lentivirus vectors under various physiological and experimental conditions, guided by the findings from earlier reports (3, 4) and our preliminary studies.

a) Adenovirus: Replication-defective adenoviral vectors expressing firefly luciferase (Fluc) (Ad5CMVLuciferase, AdFluc) and lacZ (Ad5CMVntLacZ, AdLacZ) were obtained from the Gene Transfer Vector Core at the University of Iowa (Iowa City).

b) Local uterine intraluminal infusion: Pseudopregnant animals (n=3 for each experimental condition) were injected with AdLacZ ($1X10^8$ PFU), AdFluc ($1X10^8$ PFU), or LV-Fluc/GFP ($1X10^{10}$ particles) by uterine intraluminal infusion on day 4 of

pseudopregnancy. 10 µl of PBS containing the respective virus particles was infused into the lumen of each uterine horn using a 28G1/2 needle from the oviductal end. On day 7 of pseudopregnancy (3 days after virus infusion), AdFluc- and LV-Fluc/GFP-injected animals were examined for gene expression by BLI, and the uteri from AdLacZ-injected animals were processed for LacZ staining (Supplemental Figure 1).

c) Local uterine intraluminal infusion after denudation of luminal epithelium: For effective vector delivery into subepithelial stromal cells (described below), the luminal epithelium was removed after induction of artificial decidualization and endometrial breakdown. Artificial decidualization was induced following the same protocol described previously (5). Briefly, 20 µl of sesame oil (Sigma) was injected into each uterine horn on day 4 of pseudopregnancy (day 1: vaginal plug) to induce decidualization, and animals were treated with RU486 (s.c., 3mg/kg, Sigma) on day 6 to induce endometrial breakdown. 12 hours later, a small incision was made in the uterine wall near the cervical end of each uterine horn by laparotomy. The uterine horns were gently squeezed with a pair of curved forceps in the tubo-cervical direction to remove the luminal epithelium (along with a layer of subepithelial stroma) through the incision at the cervical end. The incision was sutured after removal of the luminal epithelium. Following this procedure, the luminal epithelium was found to be completely removed, leaving the glands and stroma almost intact, by histological examination (Supplemental Figure 2).

After denudation of the uterine luminal epithelium, 100 µl of PBS containing AdLacZ ($1X10^8$ PFU, n=3), AdFluc ($1X10^8$ PFU, n=3), or LV-Fluc/GFP ($1X10^{10}$ particles n=6) virus was infused into the lumen of each uterine horn from the oviductal end using a 31G needle. Uteri from AdLacZ-injected animals were processed for LacZ staining 3 days after virus delivery. AdFluc- and LV-Fluc/GFP-injected animals were examined for transgene expression by live BLI on days 3, 7, 10, and 14 after virus delivery, and on

day 14, uteri from LV-Fluc/GFP-injected mice were excised and processed for examination of the cellular localization of GFP by IHC.

d) Induction of successive pregnancies and artificial decidualization of the uteri after local gene delivery into the endometrium:

Pregnancy: Following successful lentivirus-mediated gene delivery into the uterus by intraluminal infusion after denudation of the luminal epithelium, animals (n=12) were mated to induce pregnancy. Endometrial Fluc expression was examined in all animals on gestation days (GD) 1, 8, 12, and 19 by live BLI (6). To confirm that gene expression was confined to the endometrium: 1) live BLI of uteri was performed on GD8 by laparotomy; and 2) on GD19, BLI was performed on the uteri, placentas, and fetuses separately after removal of placentas and fetuses by caesarean section delivery. Animals were then imaged on 5 and 15 days after delivery, and pregnancy was induced again 30 days after first delivery (n=6) (6). During the second pregnancy, Fluc expression was examined by live BLI as in the first pregnancy, except without laparotomy, on GD8. Uteri were then imaged by BLI and collected 30 days after the second delivery.

Artificial decidualization: Following successful lentivirus-mediated gene delivery into the uterine stroma, another group of female mice (n=6) was mated with vasectomized males to induce pseudopregnancy and artificial decidualization (AD) in one uterine horn, leaving the other horn as a control, as described above (5). Endometrial Fluc expression was examined before AD induction (day 4 of pseudopregnancy). On day 3 after AD induction, live BLI was performed and uteri were then removed, imaged by BLI, and processed for immunohistochemical analyses. For identification of proliferating cells, all mice received BrdU (60 mg/kg) injections daily (5), starting one day after AD induction, until the day of tissue collection.

Bioluminescence Imaging

All in vivo images were acquired using the Xenogen In Vivo Imaging System (IVIS 200) under isoflurane anesthesia (1.5-2.5%), as described previously (6). Briefly, D-Luciferin (150 mg/kg body weight) was injected i.p. into anesthetized animals five minutes prior to imaging. Grayscale and pseudocolor luminescence images (blue - least intense, red - most intense) were collected and superimposed using the image-processing software Living Image 4.1 (Caliper Life Sciences) (6).

Immunohistochemistry

IHC was performed in 10 µm frozen tissue sections fixed with 4% paraformaldehyde (PFA) in PBS following our previously published procedures (5). The following primary antibodies were used for immunostaining: CD31 (1:200, rat monoclonal, BD Pharmingen), NG2 (1:500, rabbit polyclonal, Chemicon), αSMA (1:2000, mouse monoclonal, Sigma), cytokeratin 8 (1:100, rat monoclonal, National Institutes of Health developmental studies hybridoma bank), and GFP (1:1000, rabbit polyclonal, Molecular Probes). A BrdU staining kit from Zymed (Carlsbad) was used for detection of proliferating cells following the manufacturer's instructions. All specimens were visualized by immunofluorescence imaging using the respective biotinylated secondary antibodies with the Vectastain kit and fluorescein- or Texas Red-labeled avidin (Vector Laboratories). For double immunostaining, incubation with the second primary antibody was performed after staining with the first antibody and avidin-biotin blocking (Vector Laboratories). Stained sections were mounted using Vectashield mounting medium with DAPI (Vector Laboratories) and examined using a Zeiss Axioskop 2 microscope equipped with a Zeiss AxioCam camera for fluorescence or bright-field imaging (Carl Zeiss).

Alkaline Phosphatase Histochemical Staining

Trophoblast cells that line the maternal blood sinusoids (MBSs) were identified by detection of alkaline phosphatase (AP) activity using a histochemical staining method, as described previously (7). Briefly, following dewaxing and rehydration, 5 µm tissue sections (paraffin) were washed in NT solution (0.15 M NaCl; 0.1 M Tris, pH 7.5) for 20 min at room temperature (RT) followed by washing in freshly prepared NTMT solution (0.1 M NaCl, 0.1 M Tris, pH 9.5, 0.05 M MgCl2, 0.1% Tween-20, prepared fresh daily) for 10 min at RT. AP activity was visualized by incubation with a standard chromogenic AP substrate (BCIP/NBT; Promega), counterstained with Nuclear Fast Red, and mounted following dehydration and clearing through a graded series of ethanol and xylene washes.

RNA extraction and real-time PCR (qPCR)

Total RNA extraction and qPCR were performed following our previously published methods (5). QPCR was performed with the Smart Cycler® System (Cepheid) and FastStart Universal SYBR Green Master mix (Roche), and quantified using external calibration curves obtained from serial dilutions of a known number of molecules (10^2-10^9 plasmids containing beta-actin, *VEGF*, *Flt1*, *sFlt1*, *Flk1*, and *PlGF*), and all data were normalized against beta-actin. The sequences of the beta-actin, *VEGF*, *Flt1*, *sFlt1*, and *Flk1* primer pairs have been published previously.(5, 8-10) The following primers were used for *PlGF*: 5'-GGCACCACTTCCACTTCTG-3' (forward) and 5'-TCTCCTCTCCTCTCCTCTGG-3' (reverse).

In Situ Hybridization

ISH for mouse *VEGF*, *Flt1*, *sFlt1*, and human *VEGF* and *sFlt1* expression in placentas and deciduas were performed following the same procedural details and probes as described previously by us and others (5, 10-12). Frozen sections (10 µm) were hybridized with appropriate concentrations of the ^{35}S-labeled sense and antisense

probes ($5x10^6$ cpm/ml). RNaseA-resistant hybrids were detected by autoradiography, and the sections were post-stained with hematoxylin.

LacZ staining

To examine the expression of LacZ in different cell types, uteri, implantation sites, and other organs from AdLacZ-injected mice were processed for lacZ staining following a standard protocol with minor modifications (13). In brief, tissues were fixed with 4% PFA in PBS (pH 7.2) for 30 min at 4°C and washed with wash buffer (PBS containing 2 mM MgCl2, 0.01% deoxycholate, and 0.02% NP-40) for 15 min at room temperature. Samples were then stained for 16 h at 37°C with 5-bromo-4-chloro-3-indolyl-beta-D-galactopyranoside (X-gal) staining solution (wash buffer containing 1 mg/ml X-Gal, 5 mM K3Fe(CN)6 and 5 mM K4Fe(CN)6), washed in PBS, and embedded in paraffin. Serial sections were examined for X-gal staining (blue stain) after counterstaining with H&E.

Histological analysis

Tissue collection and processing for histological analysis was performed following a standard protocol, as described previously by us and others (5, 14). Briefly, tissue samples, including placentas, deciduas, and fetuses, were collected and fixed in 4% PFA overnight at 4°C. Tissues were then infiltrated and embedded in paraffin, sectioned, and stained with H&E or PAS (15). For detection of fibrin deposition in tissues, martius scarlet blue (MSB) staining was used (16).

Morphometric analysis

Diameters of fetal vessels and MBSs in the labyrinth layer were measured from CD31 fluorescently immunostained and AP histochemically-stained sections, respectively, using AxioVision 3.0 software (5). Briefly, images (40x) from the labyrinth layer were taken from at least 3 different sections for each animal. Several measurements of

vessel/MBS diameter (approximately equal measurements from wide and narrow regions) were taken, and mean diameter was calculated for each vessel/MBS.

Additionally, histological (H&E) sections were used for measurement of areas of glycogen trophoblast cells (GlyTCs), spongiotrophoblasts, and venous channels in the junctional zone. Images were captured using a Zeiss Axioskop 2 microscope equipped with a Zeiss AxioCam camera, and areas were measured using AxioVision 3.0 software (5).

Vascular density measurement

CD31, NG2, and αSMA fluorescence immunostaining were measured for calculation of an index of area density in placental sections from the control, sFlt1-shRNA, and endometrial VEGF-overexpressing animals using ImageJ software (http://rsb.info.nih.gov/ij), as described previously (5). Digital images were captured from 4 to 5 different regions of the labyrinth layer in close proximity to the chorionic plate area, and equal numbers of images were captured from the labyrinth layer in close proximity to the junctional zone in each group of animals. The distribution of intensity values in the regions of interest was visualized using the interactive 3D Surface Plot function of ImageJ. CD31-stained endothelial cells, and NG2- and αSMA-stained mural cells were distinguished from background signals by a threshold value empirically determined for each set of IHC. The densities of endothelial cells and NG2- and αSMA-positive cells in each area were calculated as the pixel values equal to or greater than the corresponding threshold. The mean values were calculated from at least 3 immunostained sections from each animal and expressed as percentages of the whole area measured in all the sections analyzed. Then the percentages represented by the NG2-positive area relative to CD31 (NG2:CD31) and the αSMA-positive area relative to CD31 (αSMA:CD31) were calculated.

Measurement of blood pressure (BP) in mice

We first measured BP using two different methods, an invasive intra-arterial method and a noninvasive tail-cuff system (17), in the same mice. Although the absolute values were different between the two methods, consistent with previous reports (17), the measurements using the tail-cuff system were significantly correlated (r=0.85, p=0.041) with the intra-arterial method, and the former method was used in all experiments in this study involving BP measurement.

The mean systolic BP was measured in conscious mice using a computerized tail-cuff method (BP-2000 Visitech System, Visitech systems Inc, Apex, NC) following the manufacturer's instructions and previous publications (17). The animals were acclimatized to the system for one week prior to initiation of the experiments, and the systolic BP was measured every alternate day at the same time of the day on a 37°C heated stage. The animals were subjected to 5 preliminary and 20 recorded measurements, and the means of 10 stable consecutive measurements were calculated.

ELISA

ELISA was performed for determination of sFlt1 and VEGF (total – free plus bound) levels in mouse serum using commercial kits from R&D Systems (Minneapolis) as previously described (1).

Western blotting

Tissue lysates from placentas and deciduas were prepared for western blotting as described previously (18). Protein concentrations in each sample were determined by the Bradford protein assay (BioRad). Samples (20 µg) were separated by SDS-PAGE and electroblotted onto nitrocellulose membranes (Amersham Pharmacia Biotech). Full-length immunoblots were used for initial optimization of each primary antibody. To avoid

variability due to membrane stripping and to efficiently use samples, blots were then cut transversely into three strips for subsequent analysis based on the molecular weight markers. The 50-250 kDa segments were used for sFlt1, Flt1, and Flk1 and were cut again from 150 to 250 kDa for longer exposure of the Flt1 band because of low signal intensity. The 25-50 kDa segments were used for beta-actin and the 15-25 kDa segments for VEGF and PlGF. The blots were blocked with 5% nonfat milk in Tris-buffered saline and incubated with the following primary antibodies at 4°C overnight: Flt1 (1:200, rabbit polyclonal, Santa Cruz), Flk1 (1:500, rat monoclonal, R&D), VEGF (1:200, rabbit polyclonal, Santa Cruz), PlGF (1:200, rat monoclonal, Santa Cruz) and beta-actin (1:500, rabbit polyclonal, Santa Cruz). After washing, primary antibodies were detected by incubation with the respective anti-rabbit or anti-rat IgGs conjugated to horseradish peroxidase (1:5000, goat polyclonal, Santa Cruz), and binding was visualized with the ECL detection system (Cell Signaling Technology). Signals were semi-quantified by densitometric analysis of bands using ImageJ (http://rsb.info.nih.gov/ij).

Mouse trophoblast stem cell culture

A trophoblast stem cell line derived from Rosa26 mice (19) was used for all experiments and was cultured and maintained as previously described (20). Cells were cultured as monolayers in medium supplemented with 25ng/ml FGF4 and 70% mouse embryonic fibroblast preconditioned medium (FCM). To promote differentiation, the FGF4 and FCM was removed and cells were then cultured for up to 6 more days with medium changed every second day. For some experiments, VEGF was added to a final concentration of 10 ng/ml (Sigma-Aldrich, Canada). RNA was isolated using RNeasy (Qiagen) and reverse transcribed using QuantiTect Reverse Transcription Kit (Qiagen). Gene expression was measured quantitatively using QuantiFast SYBR Green Mix (Qiagen) and specific primer sets for *Hprt1* as a reference gene, *Tpbpa* (marker of

spongiotrophoblast and glycogen trophoblast cells), *sFlt1* and *Flt1*. Differences were quantified using the ΔΔCT method with normalization to *Hprt1* using the following primers: *Hprt1* Forward, CCTAAGATGAGCGCGTTGAA; *Hprt1* Reverse, CCACAGGACTAGAACACCTGCTAA; *Tpbpa* Forward, AAGTTAGGCAACGAGCGAAA; *Tpbpa* Reverse: AGTGCAGGATCCCACTTGTG. All data were expressed as means ± SD using at least three samples in each experimental group. Differences between means were analyzed by one-way ANOVA and *t*-tests using GeneEx.

Supplemental figures

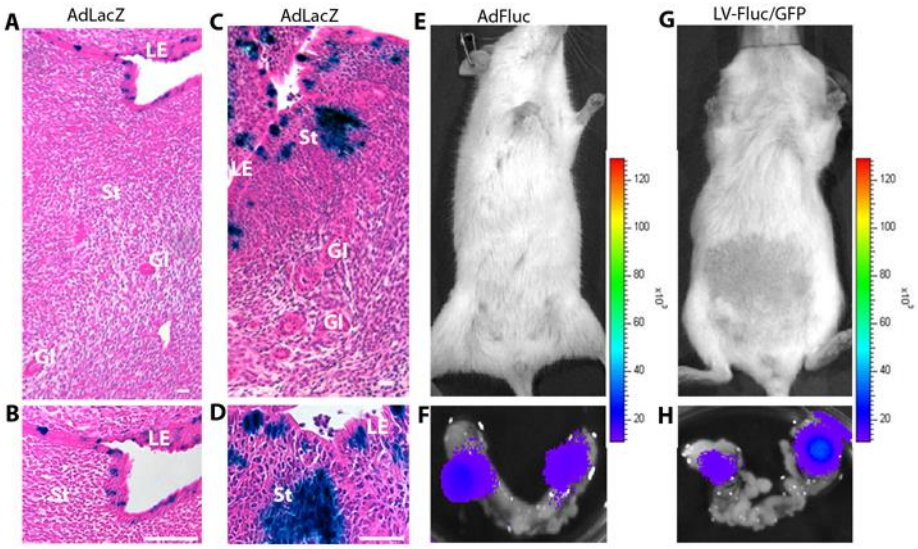

Supplemental Figure 1. Development of an endometrium-specific gene delivery method: intraluminal adenovirus infusion leads to gene expression in small, discrete patches of uterine luminal epithelial cells and in the subepithelial stroma only at sites of intraluminal injection. I. We tested local delivery of AdLacZ into the uterus by intraluminal infusion. Two different doses of AdLacZ (low = $1X10^5$ PFU and high = $1X10^8$ PFU, in 10 µl PBS) were used to infuse uterine lumens under various physiological and hormonal conditions (n=3 for each condition), including 3 days after estradiol (100 ng) treatment, 3 days after a combination of estradiol (5 ng) and progesterone (1 mg) treatment, on day 3 after artificial decidualization induction, and on day 4 of pregnancy. Uteri were examined 3 days later for transfection by LacZ staining. Interestingly, viral transfection was detected in small patches of uterine luminal epithelium only in the animals infused with the virus on day 4 of pseudopregnancy or day 4 of pregnancy (A and B). Also, in a few animals, strong LacZ staining was observed in the stromal cells immediately below the luminal epithelium (C and D), but such staining was restricted to the site of intraluminal injection. No LacZ staining was seen in the glandular epithelium or stromal cells in the deeper endometrial zones or in areas away from the injection site. There were no marked differences in the patterns of staining between the low- and high-dose-treated animals, suggesting that the number of viruses infused is not the limiting factor for transfection of uterine cells. Such differences in adenoviral transfection susceptibility in various cell types and hormonal conditions are likely due to the expression of Coxsackie adenovirus receptors (CARs) and integrins (αvb3 and αvb5) in the luminal epithelium under only certain hormonal conditions (21-24). Additionally, the basement membrane of the luminal epithelium may act as a barrier that prevents viral particles from reaching stromal cells underneath, as only stromal cells at sites of injection were infected by the virus (likely due to disruption of the luminal epithelium). II. Based on the above results (I), two groups of mice (n=3) were injected with either AdFluc ($1X10^8$ PFU) or LV-Fluc/GFP ($1X10^{10}$ particles) on day 4 of pseudopregnancy by intraluminal infusion, and reporter gene expression was examined 3 days later by BLI (E and G). No signal was detected by live BLI. When the uteri were removed and imaged, the signal was detectable only at the injection sites (F and H), indicating that the signal generated from the limited number of transfected cells at sites of injection is not sufficient for detection by live BLI. LE, Luminal epithelium; St, stromal cells; Gl, gland. Scale bars: 20 µm.

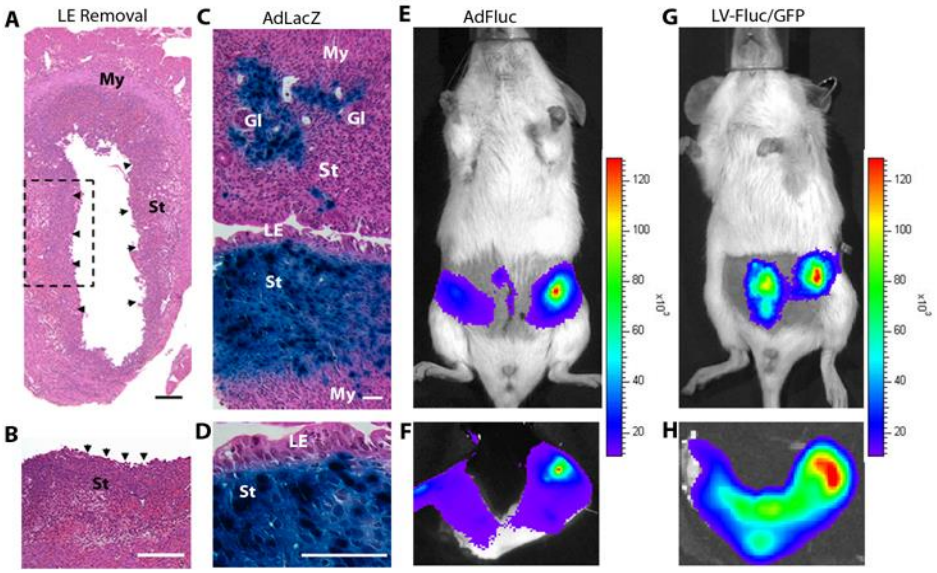

Supplemental Figure 2. Development of an endometrium-specific gene delivery method: dramatic increase in the efficiency of adenovirus- and lentivirus-mediated gene delivery into endometrial stromal cells after denudation of the luminal epithelium. After trying a variety of approaches, we successfully developed a method to reliably remove the luminal epithelium using induction of artificial decidualization and progesterone withdrawal (A and B, arrowheads), as described in the Supplementary Methods. After removal of the luminal epithelium, the animals were injected with AdLacZ, AdFluc, or LV-Fluc/GFP by intraluminal infusion. Uteri from animals treated with AdLacZ were examined for LacZ expression 3 days after intrauterine virus delivery (C and D); intense LacZ staining was evident in large patches of stromal cells throughout the uterus but not in glandular or newly formed luminal epithelial cells. Animals treated with AdFluc (E and F) or LV-Fluc/GFP (G and H) were examined for Fluc expression by BLI 3 days after virus infusion into the uterine lumen. In both groups, a very strong bioluminescent signal was observed around the uterine area (E and G), and imaging of the uteri from these animals clearly showed successful viral transfection of uterine cells (F and H). These results suggest that the luminal epithelial lining may be the primary barrier against virus delivery to underlying stromal cells. LE, Luminal epithelium; St, stromal cells; Gl, gland; My, myometrium Scale bars: 100 μm (A and B) and 20 μm (C and D).

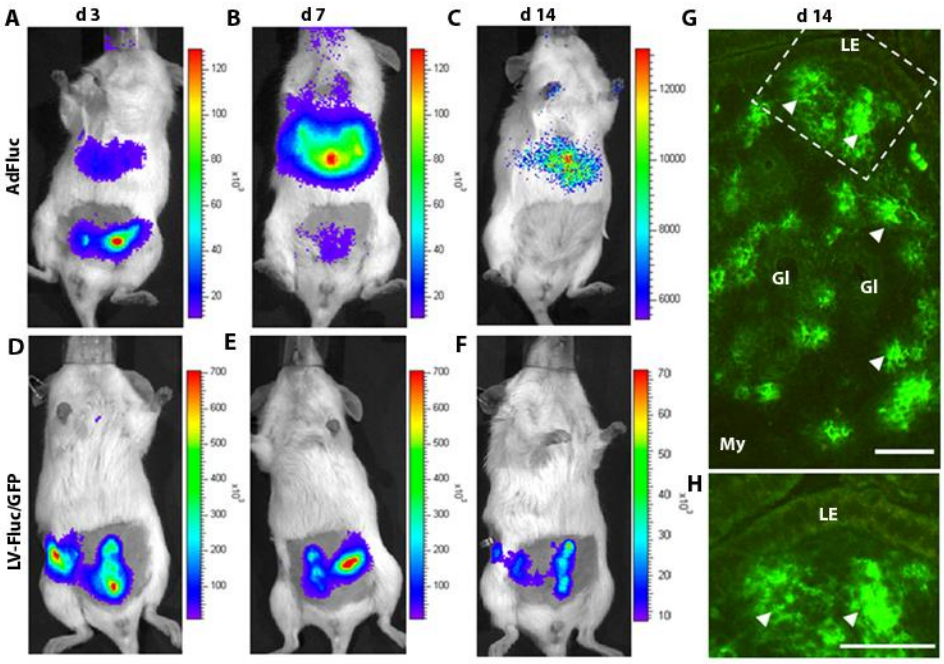

Supplemental Figure 3. Development of an endometrium-specific gene delivery method: adenovirus (AdFluc)- and lentivirus (LV-Fluc/GFP)-mediated transfection of endometrial stromal cells after denudation of the luminal epithelium. In AdFluc-injected animals (A to C), a strong Fluc signal was detected by BLI over the uterine area on day 3 after virus injection (day 0 = day of injection) (A). The signal sharply declined by day 7 (B) and was undetectable by day 14 (C). However, Fluc signal was also detected in the liver on day 3 (A), likely due to extravasation of AdFluc into systemic circulation. The signal became more intense in the liver by day 7 (B) but declined to very low levels by day 14 (C). In contrast, in LV-Fluc/GFP-injected animals, Fluc signal was evident over the uterine area from day 3 through day 14 (D to F), without any detectable signal in other organs. (G and H) Identification of LV-Fluc/GFP-transfected cells by GFP immunohistochemistry in endometrium collected on day 14. The signal was confined to stromal cells (St, arrowheads); no signal was detected in gland (GI) or luminal epithelial cells (LE). My, myometrium. Scale bars: 20 μm.

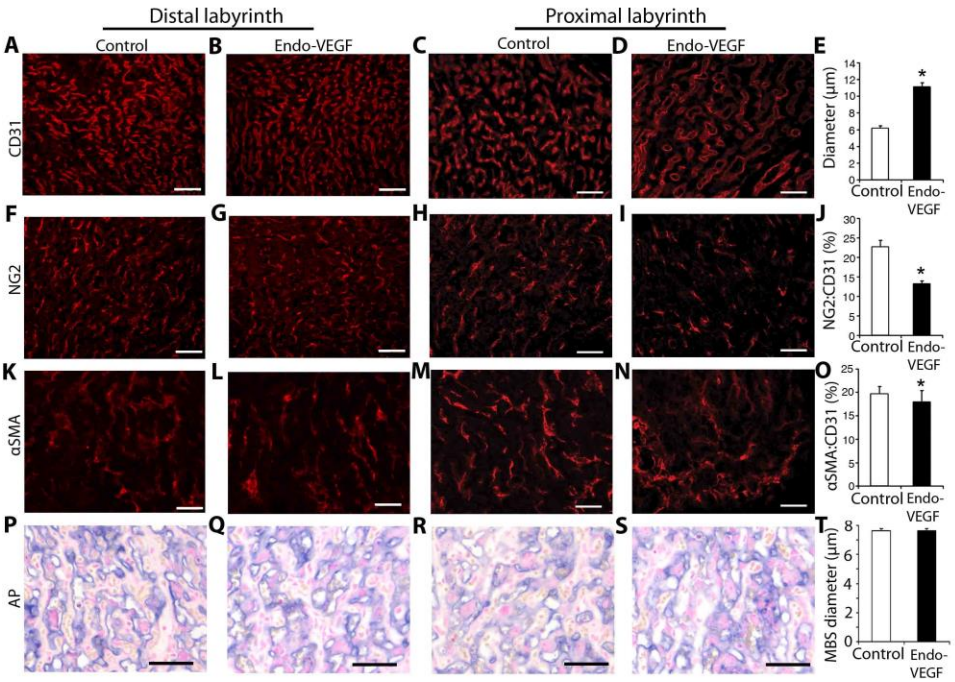

Supplemental Figure 4. Effect of endometrial VEGF overexpression during pregnancy on placental vessels. Immunofluorescence staining for endothelial cells (CD31; A to D), pericytes (NG2; F to I), and pericytes/vascular smooth muscle cells (αSMA; K to N) was performed on placental sections from control and endometrial VEGF-overexpressing animals (GD18). Because of zonal variability in the effects of different treatments in the labyrinth, fetal vessels and MBSs at close proximity to the junctional zone (proximal labyrinth; C, D, H, I, M, N, R, and S) and chorionic plate (distal labyrinth; A, B, F, G, K, L, P, and Q) were analyzed separately. Analysis of CD31 staining revealed no differences in fetal vascular density, but vessel diameters in the proximal labyrinth were significantly increased in endometrial VEGF-overexpressing placentas (C-E) relative to those in control placentas from the same region (A, B, and E). Similarly, the fractions of CD31 positive cells that were NG2 positive (J) or αSMA positive (O) (evaluated from surface plots; see Supplementary Methods) revealed no differences in the distal labyrinth, but the numbers of NG2- and αSMA-immunopositive cells in the proximal labyrinth were significantly decreased in placentas from VEGF-overexpressing animals, suggesting that the lack of pericytes/VSMCs in fetal vessels in the proximal labyrinth likely accounts for the observed dilation of vessels (E) in this zone. (P to S) Representative microphotographs of AP histochemical staining (blue) for trophoblasts lining the MBSs in the proximal and distal labyrinth. However, unlike fetal vessels, MBSs did not increase significantly in diameter in VEGF-overexpressing animals (T). Results are shown as means ± SD. *$P < 0.05$ (n = 15). Scale bars: 50 µm.

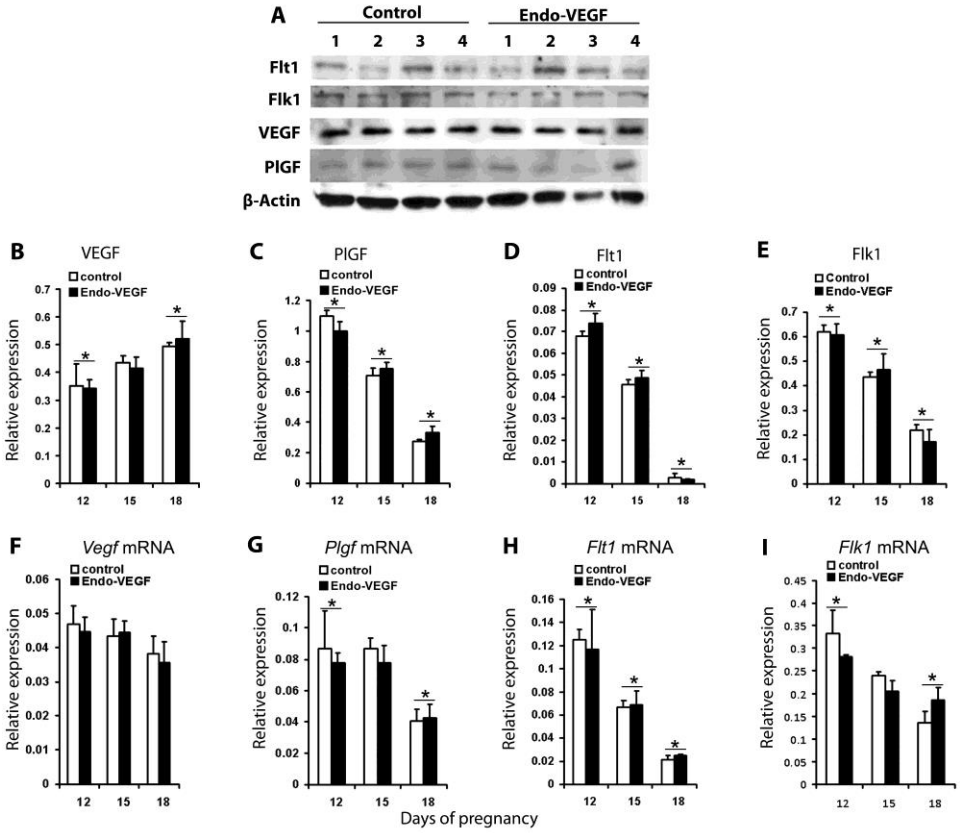

Supplemental Figure 5. No dramatic effect of endometrial VEGF overexpression on placental VEGF, PlGF, Flt1, or Flk1 expression at all stages of pregnancy. Comparison of the expression of placental VEGF (B and F), PlGF (C and G), Flt1 (D and H), and Flk1 (E and I) at both the protein level (western blot; A to E) and the RNA level (qPCR; F to I) between the placentas of control and endometrial VEGF-overexpressing animals revealed no significant changes at any stage of pregnancy. However, the placental protein and RNA levels of PlGF (C and G), Flt1 (D and H), and Flk1 (E and I) significantly decreased as pregnancy advanced from GD12 through GD18. In contrast, although placental *VEGF* mRNA levels did not change (F), VEGF protein levels (B) significantly increased from GD12 through GD18. Bar graphs (mean ± SD) with asterisks indicate significant ($P < 0.05$) difference from others (n = 5).

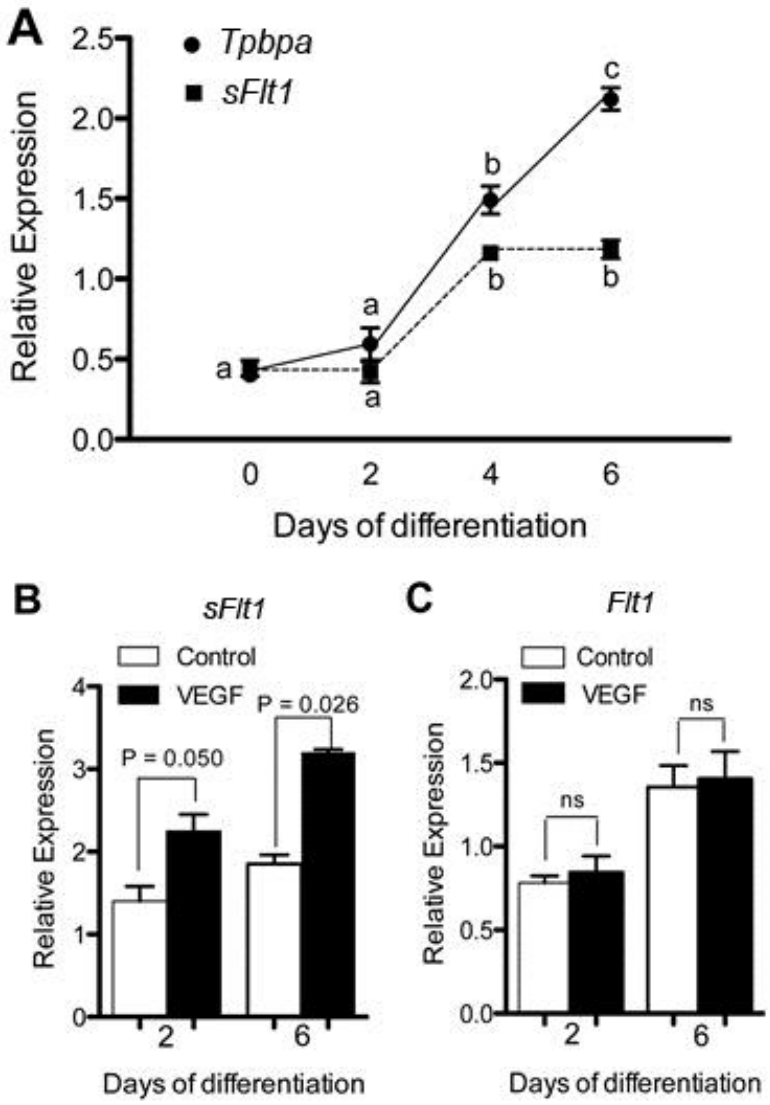

Supplemental Figure 6. VEGF promotes sFlt1 mRNA expression in cultured mouse trophoblast stem cells. (**A**) Time course of *Tpbpa* and *sFlt1* mRNA expression during trophoblast stem cell differentiation after withdrawal of FGF4 and feeder cell conditioned medium. The onset of *sFlt1* expression with *Tpbpa* fits with in vivo findings that sFlt1 is expressed in *Tpbpa*-positive spongiotrophoblast cells (10). (**B**) *sFlt1* mRNA expression is significantly stimulated by VEGF by 6 days of differentiation. However, there was no significant difference in expression of *Flt1* mRNA (**C**) between control and VEGF treated cultures. Results are shown as means ± SD. Asterisks denote $P < 0.05$.

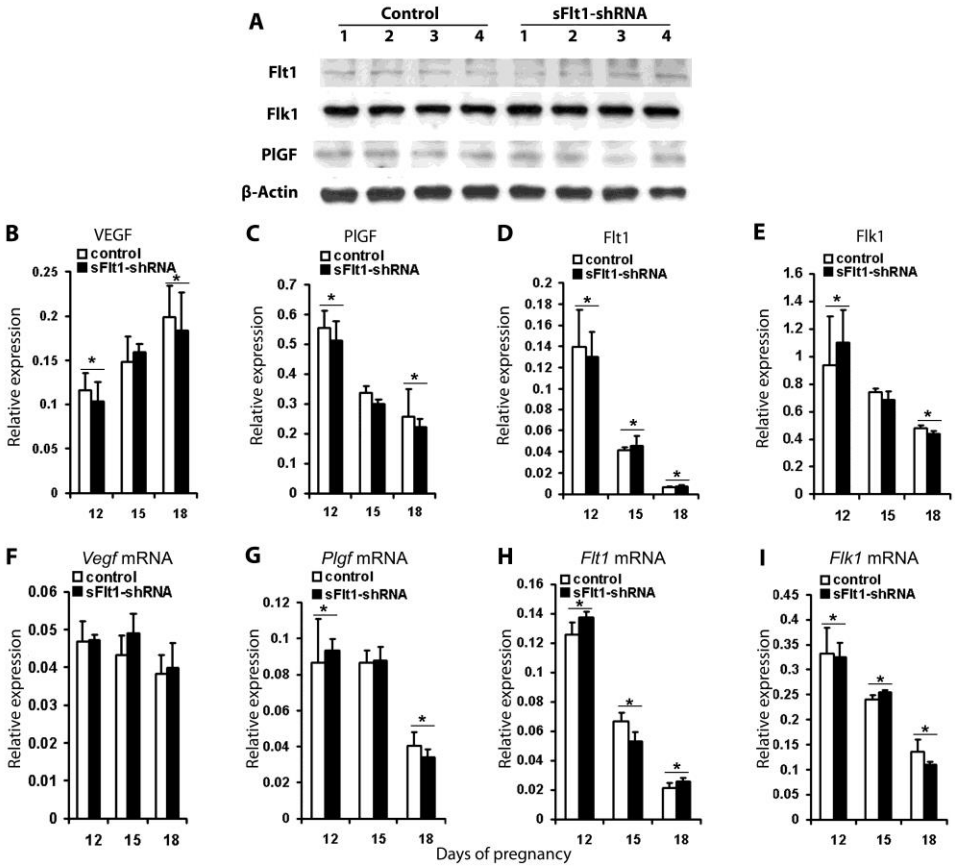

Supplemental Figure 7. VEGF, PlGF, Flt1, and Flk1 levels are unaffected by placental sFlt1 knockdown. (A) Representative western blots of control and sFlt1-shRNA-expressing placentas at GD18. (B to I) No differences in the expression of VEGF (B and F), PlGF (C and G), Flt1 (D and H), or Flk1 (E and I) were seen between control and sFlt1 knockdown placentas at either the protein level (assayed by western blotting; A to E) or the RNA level (assayed by qPCR; F to I). However, both the protein and RNA levels of PlGF (C and G), Flt1 (D and H), and Flk1 (E and I) significantly decreased between GD12 and GD18. In contrast, although *VEGF* mRNA levels did not change between GD12 and GD18 (F), VEGF protein levels increased significantly (B). Bar graphs (mean ± SD) with asterisks indicate significant ($P < 0.05$) difference from others.

Supplemental References:

1. Sung JF, Fan X, Dhal S, Dwyer BK, Jafari A, El-Sayed YY, Druzin ML, and Nayak NR. Decreased circulating soluble Tie2 levels in preeclampsia may result from inhibition of vascular endothelial growth factor (VEGF) signaling. *J Clin Endocrinol Metab.* 2011;96(7):E1148-52.
2. Dwyer BK, Krieg S, Balise R, Carroll IR, Chueh J, Nayak N, and Druzin M. Variable expression of soluble fms-like tyrosine kinase 1 in patients at high risk for preeclampsia. *J Matern Fetal Neonatal Med.* 2010;23(7):705-11.
3. Wang H, Xie H, Zhang H, Das SK, and Dey SK. Conditional gene recombination by adenovirus-driven Cre in the mouse uterus. *Genesis.* 2006;44(2):51-6.
4. Daftary GS, and Taylor HS. Reproductive tract gene transfer. *Fertil Steril.* 2003;80(3):475-84.
5. Fan X, Krieg S, Kuo CJ, Wiegand SJ, Rabinovitch M, Druzin ML, Brenner RM, Giudice LC, and Nayak NR. VEGF blockade inhibits angiogenesis and reepithelialization of endometrium. *FASEB J.* 2008;22(10):3571-80.
6. Fan X, Ren P, Dhal S, Bejerano G, Goodman SB, Druzin ML, Gambhir SS, and Nayak NR. Noninvasive monitoring of placenta-specific transgene expression by bioluminescence imaging. *PLoS One.* 2011;6(1):e16348.
7. Natale DR, Starovic M, and Cross JC. Phenotypic analysis of the mouse placenta. *Methods Mol Med.* 2006;121(275-93.
8. Takeda N, Manabe I, Uchino Y, Eguchi K, Matsumoto S, Nishimura S, Shindo T, Sano M, Otsu K, Snider P, et al. Cardiac fibroblasts are essential for the adaptive response of the murine heart to pressure overload. *The Journal of clinical investigation.* 2010;120(1):254-65.
9. Tsuda M, Iwai M, Li JM, Li HS, Min LJ, Ide A, Okumura M, Suzuki J, Mogi M, Suzuki H, et al. Inhibitory effects of AT1 receptor blocker, olmesartan, and estrogen on atherosclerosis via anti-oxidative stress. *Hypertension.* 2005;45(4):545-51.
10. He Y, Smith SK, Day KA, Clark DE, Licence DR, and Charnock-Jones DS. Alternative splicing of vascular endothelial growth factor (VEGF)-R1 (FLT-1) pre-mRNA is important for the regulation of VEGF activity. *Mol Endocrinol.* 1999;13(4):537-45.
11. Clark DE, Smith SK, He Y, Day KA, Licence DR, Corps AN, Lammoglia R, and Charnock-Jones DS. A vascular endothelial growth factor antagonist is produced by the human placenta and released into the maternal circulation. *Biol Reprod.* 1998;59(6):1540-8.
12. Simmons DG, Fortier AL, and Cross JC. Diverse subtypes and developmental origins of trophoblast giant cells in the mouse placenta. *Dev Biol.* 2007;304(2):567-78.
13. Saunders TL. Reporter molecules in genetically engineered mice. *Methods Mol Biol.* 2003;209(125-43.
14. Maynard SE, Min JY, Merchan J, Lim KH, Li J, Mondal S, Libermann TA, Morgan JP, Sellke FW, Stillman IE, et al. Excess placental soluble fms-like tyrosine kinase 1 (sFlt1) may contribute to endothelial dysfunction, hypertension,

and proteinuria in preeclampsia. *The Journal of clinical investigation.* 2003;111(5):649-58.
15. Gomoroi G. Use of the PAS technic in the pathologic laboratory. *Am J Clin Pathol.* 1955;25(11):1336.
16. Lendrum AC, Fraser DS, Slidders W, and Henderson R. Studies on the character and staining of fibrin. *J Clin Pathol.* 1962;15(401-13.
17. Krege JH, Hodgin JB, Hagaman JR, and Smithies O. A noninvasive computerized tail-cuff system for measuring blood pressure in mice. *Hypertension.* 1995;25(5):1111-5.
18. Nayak NR, Kuo CJ, Desai TA, Wiegand SJ, Lasley BL, Giudice LC, and Brenner RM. Expression, localization and hormonal control of angiopoietin-1 in the rhesus macaque endometrium: potential role in spiral artery growth. *Mol Hum Reprod.* 2005;11(11):791-9.
19. Tanaka S, Kunath T, Hadjantonakis AK, Nagy A, and Rossant J. Promotion of trophoblast stem cell proliferation by FGF4. *Science.* 1998;282(5396):2072-5.
20. Hemberger M, Hughes M, and Cross JC. Trophoblast stem cells differentiate in vitro into invasive trophoblast giant cells. *Dev Biol.* 2004;271(2):362-71.
21. Bergelson JM, Cunningham JA, Droguett G, Kurt-Jones EA, Krithivas A, Hong JS, Horwitz MS, Crowell RL, and Finberg RW. Isolation of a common receptor for Coxsackie B viruses and adenoviruses 2 and 5. *Science.* 1997;275(5304):1320-3.
22. Wickham TJ, Mathias P, Cheresh DA, and Nemerow GR. Integrins alpha v beta 3 and alpha v beta 5 promote adenovirus internalization but not virus attachment. *Cell.* 1993;73(2):309-19.
23. Aplin JD, Spanswick C, Behzad F, Kimber SJ, and Vicovac L. Integrins beta 5, beta 3 and alpha v are apically distributed in endometrial epithelium. *Mol Hum Reprod.* 1996;2(7):527-34.
24. Beauparlant SL, Read PW, and Di Cristofano A. In vivo adenovirus-mediated gene transduction into mouse endometrial glands: a novel tool to model endometrial cancer in the mouse. *Gynecol Oncol.* 2004;94(3):713-8.